ELSEVIER

Journal of Nuclear Materials 300 (2002) 65–72

journal of nuclear materials

www.elsevier.com/locate/jnucmat

Effects of nitrogen on low-cycle fatigue properties of type 304L austenitic stainless steels tested with and without tensile strain hold

Byung Sup Rho, Soo Woo Nam *,1

Department of Materials Science and Engineering, Korea Advanced Institute of Science and Technology, 373-1 Kusong-dong Yusong-gu, Taejon 305-701, South Korea

Received 12 March 2001; accepted 26 September 2001

Abstract

A quantitative analysis of the effects of nitrogen on high temperature low-cycle fatigue without and with tensile strain hold at 600 °C has been conducted for type 304L stainless steels. For better understanding of the role of nitrogen on grain boundary precipitation, the grain boundary segregation of nitrogen was analyzed by Auger electron spectroscopy. The nitrogen addition is found to give relatively better resistance to creep-fatigue than continuous low-cycle fatigue. This in turn improves the fatigue life. This is due to the retardation of the precipitation of carbides at the grain boundary and reduction in the density of grain boundary cavitation sites which are the main factor of grain boundary damage under creep-fatigue test.

1. Introduction

Type 304 stainless steels, which contain 0.08% max. carbon contents, may have grain boundary precipitation of Cr-rich carbides to deplete chromium content in the vicinity of the grain boundaries. In applications under corrosive environments, this Cr-depletion region around the grain boundaries reduces the resistance to intergranular stress corrosion cracking. However, it has been reported that the reduction of the carbon content of the stainless steel can effectively increase the resistance to grain boundary sensitization of stainless steels [1]. Consequently, the L-grades of low carbon austenitic stainless steels have been developed for use in corrosive environments. However, the low carbon content of this steel results in a relatively low yield strength and consequently limits their applications. In an attempt to overcome this disadvantage, addition of nitrogen to austenitic stainless steel has been implemented for use as a structural material in reactors because nitrogen-added stainless steel has superior mechanical properties in comparison with conventional L-grades stainless steel [2–5].

304L and 304NG (nitrogen-added) austenitic stainless steels are of considerable interest for liquid-metal fast-breeder reactor (LMFBR) structural component design because of their resistance to neutron irradiation, excellent toughness, and weldability. In this application, the materials of the components are subjected to cyclic thermal stresses induced by temperature gradient as a result of start-ups, operation, and shut-downs. Therefore, high temperature low-cycle fatigue represents a predominant failure mode, necessitating significant consideration in the design and life analysis of such components.

It has been found in previous work that the addition of nitrogen to austenitic stainless steels inhibits cross-slip and climb of dislocations, therefore, favors planar slip

* Corresponding author. Tel.: +82-42 869 3318; fax: +82-42 869 3310.

E-mail address: namsw@cais.kaist.ac.kr (S.W. Nam).

[1] Jointly appointed at the Center for the Advanced Aerospace Materials.

0022-3115/02/$ - see front matter
PII: S0022-3115(01)00709-7

[6]. Also, the increase in fatigue strength is explained by the nitrogen influence with promoting planar slip and thus slip reversibility according to a lowering influence of nitrogen on the stacking fault energy [7]. It has been reported that in elongated Cr–Ni austenitic stainless steels, nitrogen atoms associated with chromium atoms interact with dislocations [8], and the nitrogen atoms are attracted to the short range ordered Fe–Cr regions, which lead to a change in the dislocation structure.

Under total axial strain control mode, it has been found that the fatigue lives of austenitic stainless steels at room temperature and at 600 °C were improved by the addition of nitrogen, and the fatigue life increased with increasing nitrogen content up to 0.12% [9]. However, in tensile strain hold-time tests, higher nitrogen content has an adverse effect, which has been explained to be a consequence of high stress concentration in the grain boundary regions caused by the inhibition of recovery of matrix substructure and the planar slip induced by the addition of nitrogen [10]. But, because of the difficulty in explaining both the interaction between nitrogen atoms and dislocation and the roles of nitrogen near the grain boundaries, the effects of nitrogen on low-cycle fatigue properties in austenitic stainless steels are not clearly understood.

In the present paper, to gain a better understanding of the role of the nitrogen element on high temperature low-cycle fatigue in type 304L austenitic stainless steels, a comparison of fatigue properties with and without the nitrogen element was carried out. Furthermore, in order to investigate the effect of the nitrogen element on high temperature low-cycle fatigue with strain hold, creep-fatigue interaction tests at 600 °C were conducted. For the consideration of the nitrogen segregation on the influence of the grain boundary precipitation, some studies in the grain boundary segregation by means of Auger electron spectroscopy (AES) were performed.

2. Experimental method

2.1. Materials

The chemical compositions of the as-received 304L (0.03% N) and 304NG (0.08% N) stainless steels used in the present investigation are given in Table 1. The heat treatments of the as-received alloys were conducted at 1050 °C for 25.6 min. The longitudinal axis of most specimens was in parallel to the direction of rolling.

2.2. Low-cycle fatigue tests

Cylindrical specimens having 8 mm gauge length and 7 mm diameter were cyclically fatigued in air under axial strain control using a servohydraulic testing machine, Instron model 1350. A symmetric triangular wave shape was used with a strain rate of 4×10^{-3} s^{-1}. A total strain range of ±1.0–2.0% was used in low-cycle fatigue tests at 600 °C. Creep-fatigue tests were conducted with a hold at the tensile peak strain for 20 min. The stress axis under low-cycle fatigue tests is parallel to the rolling direction.

For high temperature fatigue tests, a radiant furnace was used to heat the specimen and the test temperature was controlled at 600 °C. The fatigue life (N_f) was defined as the number of cycles at which the saturated tensile load decreased by 20% [11,12].

2.3. Observation of microstructure

The microstructures of the LCF tested specimens were investigated using scanning electron microscopy (SEM) and transmission electron microscopy (TEM). For optical microscopy, the samples were ground using 220–2000 grit emery paper and then mechanically polished using 0.05 μm alumina. After the fatigue tests, the specimen surface and the fractured surface were examined by SEM. For observing the microstructure by TEM, the specimens were initially thinned mechanically to 50 μm, and then electropolished by Bolman treatment in a solution of nitric acid 30% and methanol 70% at 8–15 V and below −40 °C.

2.4. Auger spectroscopy analyses

In order to investigate the grain boundary segregation of nitrogen, microchemistry at the grain boundary was studied using a PHI Model 4300 scanning Auger electron spectroscope. After the low-cycle fatigue tests of 304L and 304NG stainless steels at 600 °C, fractured facets were obtained by impact fracture at liquid nitrogen temperature (LNT). The facets of the rupture surface were analyzed in the Auger vacuum chamber after sputter-cleaning. The acceleration voltage of the primary electron beam was 10 kV. The testing chamber itself was capable of achieving a high vacuum of 10^{-10} Torr using a diffusion pump, but the vacuum during the analysis was about 10^{-8} Torr.

Table 1
Chemical composition of 304L and 304NG stainless steels (in wt.%)

Alloy	C	Si	Mn	P	S	Ni	Cr	Mo	Cu	N
304L	0.029	0.57	1.05	0.020	0.003	10.13	18.0	0.07	0.19	0.03
304NG	0.019	0.52	1.02	0.024	0.002	9.64	18.5	0.06	0.11	0.08

3. Results and discussion

3.1. Microstructures prior to low-cycle fatigue tests

The optical microstructures of the as-received 304L and 304NG stainless steels are shown in Fig. 1. The average grain size of both stainless steels is about 60 μm. The δ-ferrite, which is shown as the dark area in the figures, was observed to be of narrow bamboo morphology running in parallel to the rolling direction. The amounts of δ-ferrite in the 304L and 304NG stainless steel were measured to be 0.99% and 0.33%, respectively using the ferritescope. This is known from the phase diagram since nitrogen is an austenite stabilizer. Thus the amount of δ-ferrite in 304NG stainless steel is less than that of δ-ferrite in 304L stainless steel.

3.2. Tensile tests

To investigate the tensile properties of 304L and 304NG stainless steels at 600 °C, tensile tests were performed in air at a strain rate of 4×10^{-3} s^{-1}. The same rate was used for continuous low-cycle fatigue. Yield stresses, ultimate tensile stresses and elongations for both stainless steels are compared in Table 2. The 304NG stainless steel, due to the effect of the solid solution hardening by the nitrogen element, showed higher yield stress and ultimate tensile stress than 304L stainless steel, as reported by other researchers [5,13,14]. However, the elongation of the 304NG stainless steel is lower than that of the 304L stainless steel. The decrease of ductility due to the addition of nitrogen is consistent with other data [5].

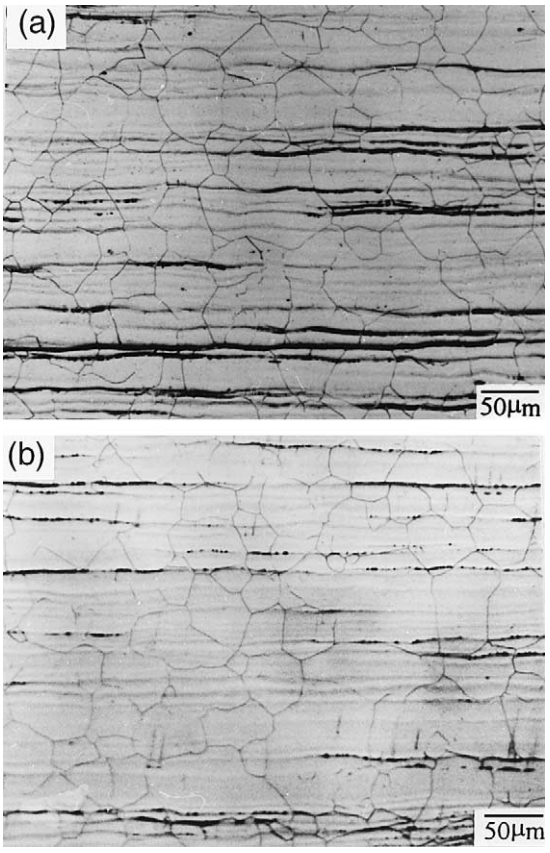

Fig. 1. Optical micrographs of two alloys before low-cycle fatigue testing: (a) 304L and (b) 304NG.

Table 2
Comparison of tensile properties of 304L and 304NG stainless steels at 600 °C

Alloy	YS (MPa)	UTS (MPa)	Elongation (%)
304L	122	334	44.6
304NG	134	352	41.6

3.3. Low-cycle fatigue tests

Even though cyclic plastic strain is a measurable physical quantity that can be directly related to fatigue damage, the Coffin–Manson (plastic strain range–fatigue life) relationship lacks a means to explain the difference in fatigue properties due to the relative difference in cyclic fatigue strengths of both stainless steels. Therefore, it is thought to be reasonable to utilize an energy-based parameter as fatigue damage, which is referred to the maximum hysteresis loop energy per cycle [15,16].

Fig. 2 represents the relationship between the hysteresis loop energy and the number of cycles to failure of 304L and 304NG stainless without and with tensile strain hold at 600 °C. In the case of continuous low-cycle fatigue, the 304L stainless steel fatigue life showed longer than that of the 304NG stainless steel. Since continuous low-cycle fatigue life is a function of the ductility of the material, lower fatigue life of the 304NG stainless steel compared with that of the 304L stainless steel can be inferred reasonably from results of the tensile tests. Similar results [17] have been reported that the fatigue life of phosphorus-doped 304L under continuous low-cycle fatigue is shorter than that of commercial 304L stainless steel, owing to the decrease in ductility and the increase of strength by phosphorus additions.

With a tensile strain hold, the 304NG stainless steel showed better resistance to creep fatigue than the 304L stainless steel. However, the fatigue lives of both stainless steels with a tensile strain hold of 20 min were lower in comparison with that of continuous low-cycle fatigue. The 304NG stainless steel showed a smaller reduction of fatigue life than the 304L stainless steel under a tensile strain hold.

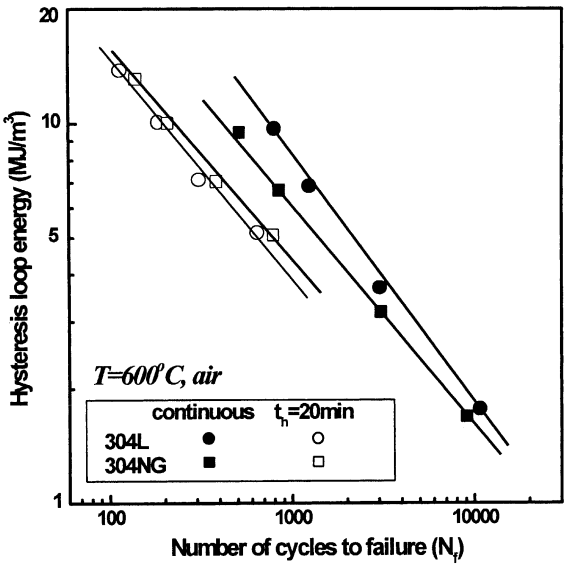

Fig. 2. Results of low-cycle fatigue tests with and without tensile strain hold for 304L and 304NG stainless steels at 600 °C in terms of hysteresis loop energy.

In an earlier paper [18], nitrogen-added 316L showed longer fatigue lives than 316 stainless steel under continuous low-cycle fatigue. Furthermore, according to the results of Nilsson [18], the tensile hold time sensitivity under creep-fatigue is higher in nitrogen-added steel, 316LN than in 316 stainless steel. This finding for the type 316 stainless steels is in conflict with the present results for the type 304 stainless steels. Therefore, it is necessary to investigate the close correlation between the fatigue resistances with and without tensile strain hold and the microstructural aspects of the fatigue deformation.

3.4. Observation of fatigue fracture surface and microstructure

It has been pointed out that addition of nitrogen facilitates the occurrence of planar slip in austenitic stainless steels [5,8,19]. Vogt et al. [5] has observed that in 316LN austenitic stainless steel under continuous low-cycle fatigue, dislocation arrangement transformed to a planar structure, and fatigue crack growth rate decreased from 350 to 573 °C when 0.2% nitrogen is added to the stainless steel. The planar arrangement of dislocation means that it is more difficult to cross slip in nitrogen-added 316L than in regular 316L stainless steels. It is considered that the difficulty to cross slip in nitrogen-added stainless steel lowered the fatigue crack growth more than that of nitrogen-free stainless steel. However, the dislocation arrangements such as planar slip were not found in continuous low-cycle fatigue of 304NG stainless steel as shown in Fig. 3(a).

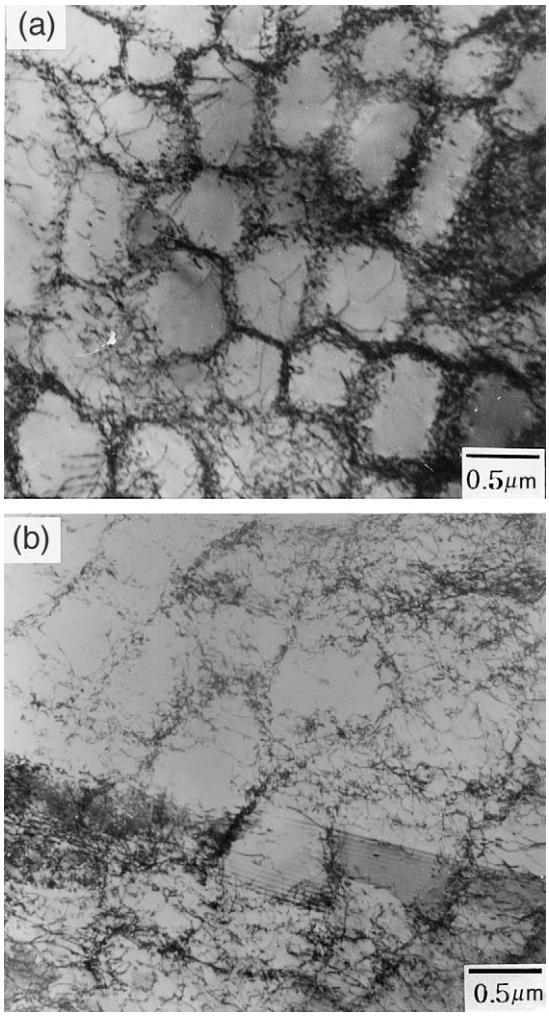

Fig. 3. Transmission electron micrographs of 304NG stainless steel subjected to low-cycle fatigue testing (a) without tensile strain hold and (b) with tensile strain hold.

On the other hand, result of creep-fatigue tests on 316LN stainless steel at 600 °C [10] shows that planar slip induced under creep-fatigue interaction tends to enhance the stress concentration in the immediate vicinity of grain boundaries and promotes the intergranular fatigue fracture, leading to a decrease in fatigue life. However, the dislocations induced in 304NG stainless steel after low-cycle fatigue forms a cell structure regardless of testing with or without tensile strain hold, as shown in Fig. 3(b). Despite addition of nitrogen to 304L stainless steel and after creep-fatigue testing at 600 °C, cell structure was found predominant but no evidence of planar slip. This means that there were different mechanisms of the nitrogen effects causing the planar slip and

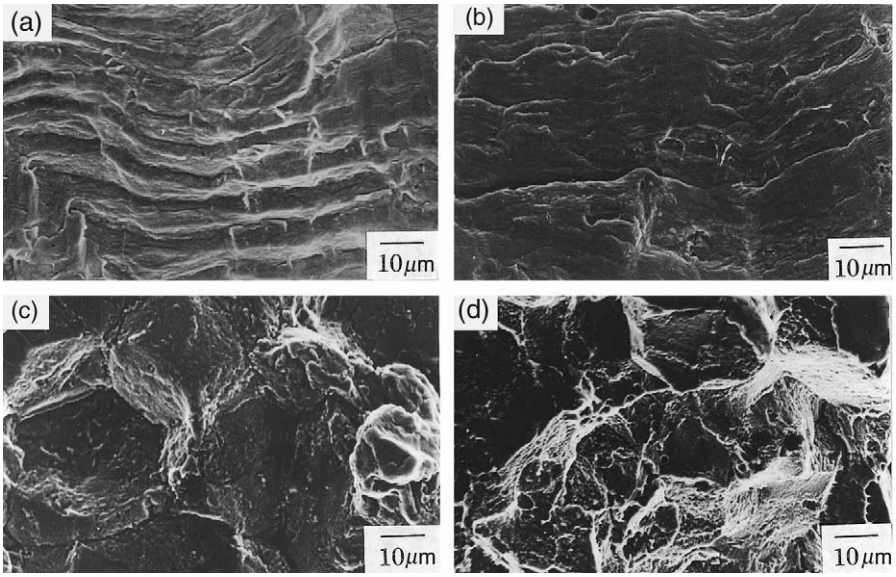

Fig. 4. Comparison of fatigue fracture surfaces of two stainless steels tested at 600 °C. (a) 304L after continuous cyclic fatigue test ($\Delta\varepsilon_t = \pm 2.0\%$), (b) 304NG after continuous cyclic fatigue test ($\Delta\varepsilon_t = \pm 2.0\%$), (c) 304L after creep-fatigue test ($\Delta\varepsilon_t = \pm 2.0\%$), and (d) 304NG after creep-fatigue test ($\Delta\varepsilon_t = \pm 2.0\%$).

the stress concentration at the grain boundaries for inducing the intergranular fatigue fracture.

In order to investigate the fatigue mechanisms in the 304 stainless steels, detailed SEM studied on fracture surfaces were carried out. Fig. 4 shows the fracture surfaces of 304L and 304NG under low-cycle fatigue testing with and without tensile strain hold. In the case without tensile strain hold, both stainless steels reveal transgranular fatigue fracture with representative striations. This indicates that fatigue cracks initiate from the specimen surface and the crack propagated in a transgranular manner.

On the other hand, the fatigue fracture surfaces of 304L and 304NG after the creep-fatigue tests show intergranular fatigue fracture, as shown in Figs. 4(c) and (d). This means that the grain boundary damage during the tensile strain hold is detrimental compared to that accumulated during continuous cycling, and the grain boundary became weaker than the matrix due to the tensile strain hold. However, as shown in Fig. 2, the 304NG stainless steel has a longer fatigue life than the 304L stainless steel under creep-fatigue condition. Therefore, it is necessary to investigate the intergranular fractured facets and microstructures of the specimens tested under creep-fatigue.

Reasonable insight can be gained to aid in understanding of the difference in creep-fatigue behaviors in the 304 stainless steels by examining the microstructural features of the fractured surfaces at high magnification, as shown in Fig. 5. In the high magnification, both stainless steels with tensile strain hold show grain boundary cavities at the facets of the intergranular fractures. The 304NG stainless steel (Fig. 5(b)) shows a

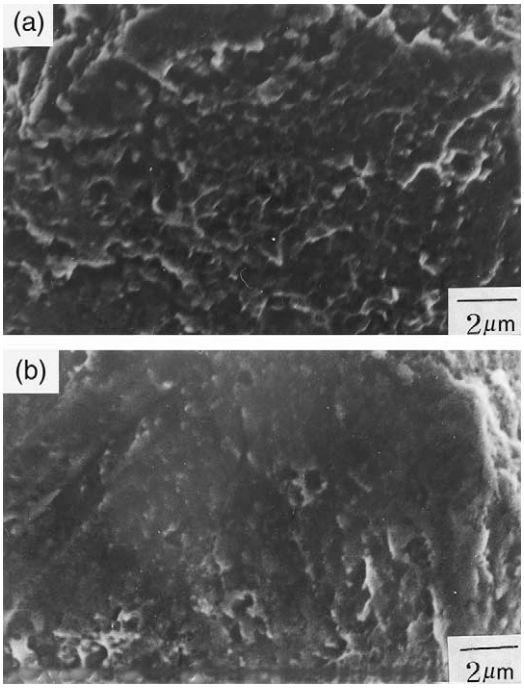

Fig. 5. Scanning electron micrographs showing the density of cavities on the grain boundary facet from the LNT fracture surface for two stainless steels after creep-fatigue testing at 600 °C ($\Delta\varepsilon_t = \pm 2.0\%$): (a) 304L and (b) 304NG.

relatively lower density of cavity than the 304L (Fig. 5(a)) tested at the same strain range. Furthermore, this trend in the cavity density is consistent at every strain range tested.

Many investigations [20–25] showed that the main damage of creep-fatigue in austenitic stainless steels is mainly attributed to the nucleation and growth of cavities at grain boundary and enlargement into intergranular cavities and cracking during tensile strain hold time. According to other studies [22,26], the grain boundary carbide is a site conducive to formation of the cavities at the grain boundary, and the cavity density at the grain boundary is very closely related to the density of the carbides, which play a key role in creep-fatigue behavior of austenitic stainless steels. Fig. 6 shows that the density of carbides in the 304NG stainless steel is lower than that of the 304L stainless steel. This implies that the 304NG stainless steel has lower cavity density at the grain boundary than the 304L stainless steel. This indicates that the addition of nitrogen in austenitic stainless steels reduces the density of carbide at the grain boundary. Some researchers [27,28] reported that the addition of nitrogen in austenitic stainless steels retarded the precipitation and growth of grain boundary carbides. Therefore, it is important to investigate the distribution of nitrogen on grain boundary precipitation, using AES analyses.

3.5. Auger analysis results

Figs. 7(a) and (b) shows the Auger spectra obtained from fatigue fracture surfaces of the 304L and 304NG, respectively. These spectra correspond to chemical analyses performed at the intergranular facet areas. The Auger peaks for the main constituents, iron, chromium, and much weaker, nickel and carbon, are clearly seen. Two spectra differing from each other by nitrogen are observed at the intergranular fatigue fracture facets. The 304L stainless steel show very weak spectra of nitrogen on the grain boundaries, while 304NG show well manifested spectra of nitrogen.

The intensity of the Auger transitions is a relative measure of the concentration of the respective elements on the fractured surface. However, an accurate calculation of the concentrations near the fractured surface from Auger peak areas can be performed if a detailed knowledge of the depth distribution of the elements is available. Fig. 8 shows the Ar^+ ion sputter depth profiles in order to obtain additional information concerning the depth distribution of nitrogen segregation and chromium near the grain boundaries. The results shown in Fig. 8 represent that the concentration of nitrogen at a point nearest to the grain boundaries is very high compared with that in the interior region away from the grain boundary. A sputtering time increases, the concentration

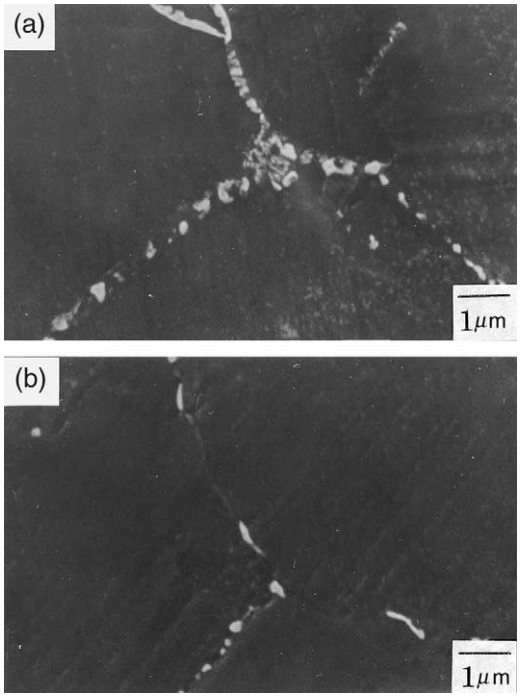

Fig. 6. Scanning electron micrographs showing the density of grain boundary carbide for two stainless steels after creep-fatigue testing at 600 °C ($\Delta\varepsilon_t = \pm 2.0\%$): (a) 304L and (b) 304NG.

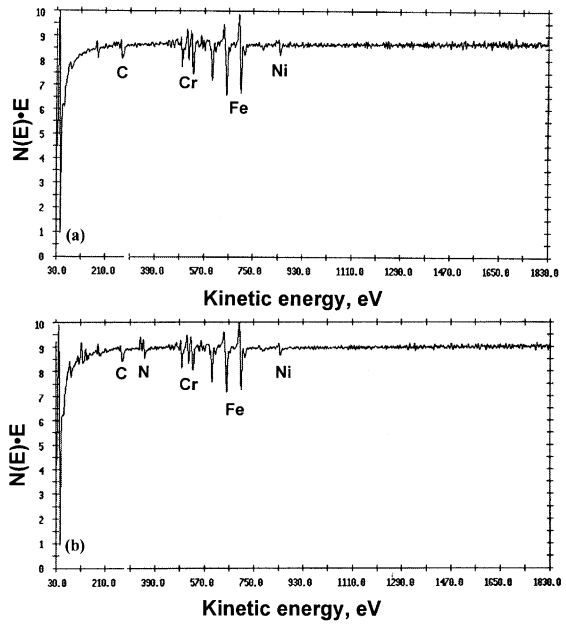

Fig. 7. Auger spectra obtained from the grain boundary facet after creep-fatigue testing at 600 °C ($\Delta\varepsilon_t = \pm 2.0\%$): (a) 304L and (b) 304NG.

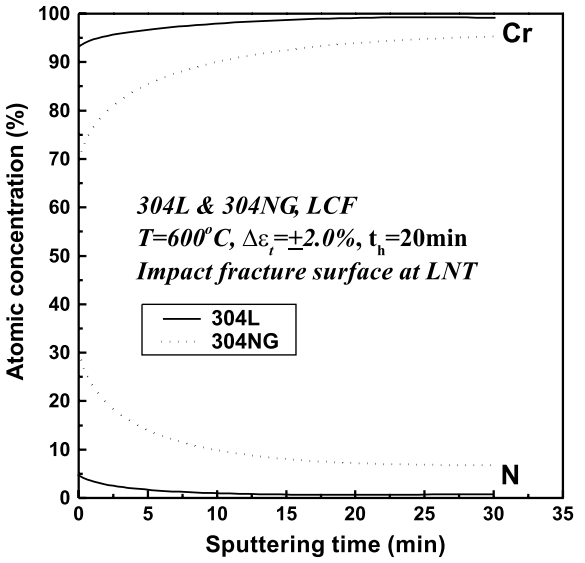

Fig. 8. Ar^+ ion depth profiles of the chromium and nitrogen, showing the grain boundary segregation near the grain boundary after creep-fatigue testing on 304L and 304NG stainless steels at 600 °C.

of nitrogen decreased rapidly until a steady-state is reached. This implies that the segregation of nitrogen toward the grain boundaries is induced by a preferential process associated with the diffusion of interstitials during high temperature low-cycle fatigue. On the other hand, the amount of chromium element at the grain boundaries is very low compared with that in the interior region, and the concentration of chromium away from the grain boundaries increased with increasing sputtering time. It is likely that the low concentration of chromium at the grain boundaries makes the formation of grain boundary Cr-rich carbides difficult. It has been reported [28] that the nitrogen atoms being segregated to the grain boundaries form a shell around the carbides, which would act as a barrier to hinder the transport of chromium from the austenitic matrix into the carbide across the austenite–carbide interface.

Fig. 8 shows that the profiles of the concentrations of nitrogen and chromium from the grain boundaries in the 304NG changed drastically relative to the changes in concentration of both elements in the 304L. The concentration of chromium in the 304NG is lower than that in the 304L. This implies that the formation of Cr-rich carbides at the grain boundary in the 304NG is more limited than that in the 304L, which has a small amount of nitrogen at the grain boundaries.

Generally, overwhelming segregation elements, such as sulfur and phosphorus, acting through selective segregation at the internal free surface can play a key role in cavitation in nickel, nickel-based superalloys [29,30] and ferritic steels [31]. In a recent study on creep behavior of 304 stainless steel, segregation of phosphorus at grain boundaries showed to accelerate the cavity nucleation rate at the grain boundary [32]. Furthermore, it has been reported that since phosphorus-doped 304L stainless steel lowers the nucleation and growth rate of cavity at the grain boundary, the creep-fatigue life of phosphorus-doped 304L is longer than that of commercial 304L stainless steel tested at 550 °C [33,34].

Observations of microstructures with reference to Auger spectra analyses suggest that the 304NG has a lower tendency of intergranular fatigue cracking than the 304L under creep-fatigue conditions, because the 304NG has a smaller amount of grain boundary carbides than the 304L. This is believed due to the segregation of nitrogen to the grain boundary. As discussed earlier, the main creep-fatigue damage in austenitic stainless steels is attributed to the grain boundary carbides which are the sites for grain boundary cavitation. Therefore, the resistance to the intergranular damage of type 304L stainless steel (Fig. 5(a)) under creep-fatigue can be improved by adding nitrogen, but not without a penalty in lower fatigue life for the 304NG compared to that for the 304L under the continuous cyclic fatigue condition.

4. Conclusions

An experimental study of high temperature low-cycle fatigue with and without tensile strain hold on 304L and 304NG stainless steels leads to the following conclusions:

1. The effect of nitrogen addition on the low-cycle fatigue behavior of type 304L stainless steels at 600 °C is found to give good fatigue resistance under creep-fatigue but poor results under continuous low-cycle fatigue. This is because the mechanisms for fatigue crack nucleation and propagation are different in both cases, i.e. a transgranular manner under continuous low-cycle fatigue and a intergranular manner under creep-fatigue.

2. Type 304NG stainless steel showed that addition of nitrogen has improved the fatigue life under creep-fatigue. This is intimately related to the grain boundary cavitation due to the precipitation of carbides at the grain boundary rather than the change of dislocation structure related with planar slip. Since addition of nitrogen retards the formation of Cr-rich carbides at the grain boundary, the 304NG compared to the 304L has lower grain boundary cavitation, showing the good resistance under creep-fatigue.

Acknowledgements

The authors would like to express their appreciation to POSCO for the financial support of this study and to Technical Research Laboratories, POSCO for supplying the specimens.

References

[1] D. Pickering, I.M. Bernstein, in: Handbook of Stainless Steels, McGraw-Hill, New York, 1974, p. 16.
[2] K.J. Irvine, T. Gladman, F.B. Pickering, J. Iron Steel Inst. 207 (1969) 1017.
[3] R.E. Stoltz, J.B. Vander Sande, Metall. Trans. A 11 (1980) 1033.
[4] J.O. Nilsson, J.B. Vander Sande, Fatigue Eng. Mater. Struct. 7 (1984) 55.
[5] J.B. Vogt, J. Foct, C. Regnard, G. Robert, J. Dhers, Metall. Trans. A 22 (1991) 2385.
[6] J.O. Nilsson, Scripta Metall. 17 (1983) 593.
[7] S. Degallaix, G. Degallaix, J. Foct, in: Proceedings of Conference on Low Cycle Fatigue and Elasto-Plastic Behavior of Materials, Elsevier, Amsterdam, 1987, p. 83.
[8] J.B. Vogt, T. Magnin, J. Foct, Fatigue Fract. Eng. Mater. Struct. 16 (1993) 555.
[9] S. Degallaix, G. Degallaix, J. Foct, in: ASTM STP 942, American Society for Testing Materials, Philadelphia, PA, 1988, p. 798.
[10] J.O. Nilsson, in: ASTM STP 942, American Society for Testing Materials, Philadelphia, PA, 1988, p. 543.
[11] S.W. Nam, J.W. Hong, K.T. Rie, Metall. Trans. A 19 (1988) 121.
[12] J.J. Kim, S.W. Nam, Scripta Metall. 23 (1989) 1437.
[13] M.L.G. Byrnes, M. Grujicic, W.S. Owen, Acta Metall. 35 (1987) 1853.
[14] A. Soussan, S. Degallaix, T. Magnin, Mater. Sci. Eng. A 142 (1991) 169.
[15] C.E. Feltner, J. Morrow, Trans. ASME Ser. D 83 (1961) 15.
[16] A. Saxena, S.D. Antolovich, Metall. Trans. A 6 (1975) 1809.
[17] J.J. Kim, S.W. Nam, Scripta Metall. 23 (1989) 1437.
[18] J.O. Nilsson, Fatigue Eng. Mater. Struct. 7 (1984) 55.
[19] P.R. Swann, Corrosion 19 (1963) 102.
[20] P.S. Maiya, S. Majumdar, Metall. Trans. A 8 (1977) 1651.
[21] J.W. Hong, S.W. Nam, K.T. Rie, J. Mater. Sci. 20 (1985) 3763.
[22] S.W. Nam, Y.C. Yoon, B.G. Choi, J.J. Kim, J. Mater. Sci. 31 (1996) 4957.
[23] R. Hales, Fatigue Eng. Mater. Struct. 3 (1980) 339.
[24] D.S. Wood, J. Wynn, A.B. Baldwin, P. O'riordan, Fatigue Eng. Mater. Struct. 3 (1980) 39.
[25] P.S. Maiya, Mater. Sci. Eng. 47 (1981) 13.
[26] R.G. Fleck, D.M.R. Taplin, C.J. Beevers, Acta Metall. 23 (1975) 415.
[27] C.L. Briant, Scripta Metall. 21 (1987) 71.
[28] T.A. Mozhi, H.S. Betrabet, V. Jagannathan, B.E. Wilde, W.A.T. Clark, Scripta Metall. 20 (1986) 723.
[29] W.C. Johnson, J.E. Doherty, B.H. Kear, A.F. Giamei, Scripta Metall. 8 (1974) 971.
[30] R.T. Holt, W. Wallace, Inter. Metall. Rev. 21 (1976) 1.
[31] S.H. Chen, T. Takasugi, D.P. Pope, Metall. Trans. A 14 (1983) 571.
[32] J.H. Hong, S.W. Nam, S.P. Choi, J. Mater. Sci. 21 (1986) 3966.
[33] Y.C. Yoon, J.J. Kim, D.M. Wee, S.W. Nam, J. Kor. Inst. Met. Mater. 30 (1992) 1401.
[34] J.J. Kim, S.W. Nam, in: Proceedings of the Eighth Biennial European Conference on Fracture (ECF8), Chameleon, London, 1990, p. 1217.